

GO4RL: IMPROVING THE PRE-TRAINING DATA MIXTURE OF LARGE LANGUAGE MODELS FOR ENHANCING REINFORCEMENT LEARNING

Anonymous authors

Paper under double-blind review

ABSTRACT

The development of reinforcement learning (RL)-trained large language models (LLMs) such as OpenAI-o1 and DeepSeek-R1 has demonstrated notable advancement in solving complex logical tasks involving mathematics and programming. Existing studies, however, show that the reasoning capability of RL-trained LLMs varies across base model families, raising the critical research question: what base model is suitable for augmenting RL’s reasoning capabilities? Recent prevailing research shows that 1) the reasoning capacity of the RL-trained model remains bounded by that of its base model and 2) the data mixture used for pre-training has a significant impact on the base model’s performance. Building on these insights, we propose Go4RL, which seeks to answer the above question by investigating how pre-training dataset mixture strategies relate to a viable base model for RL training. Go4RL first defines the measurement of base models’ reasoning capability boundaries as the average perplexity scores of the base LLM on the RL-generated k responses, denoted by $\text{avg}(k\text{-ppl})$. Then we formulate finding the optimal pre-training dataset mixing ratios for RL as a regression task, using the proposed $\text{avg}(k\text{-ppl})$ as the fitting objective instead of the traditional language modeling loss. Finally, we use the learned regression model to predict the performance of unseen mixtures and apply the best predicted mixture to train a large-scale model that achieves better RL performance. We train both pre-trained and RL-trained proxy models with 1M parameters for regression fitting and then scale up to 1B parameters using various data mixtures to validate Go4RL. The experimental results on both online and offline RL algorithms show that the optimized data mixture predicted by Go4RL yields a better base model for RL training.

1 INTRODUCTION

The recently released large language models (LLMs), including OpenAI-o1 (Jaech et al., 2024) and DeepSeek-R1 (Guo et al., 2025), have demonstrated superior skill in accomplishing intricate reasoning tasks, particularly in mathematics and programming. The key to these advancements is reinforcement learning (RL) with verified rewards or human preferences, which has emerged as a pivotal phase in the post-training process of the base LLM for establishing enhanced reasoning abilities (Dang et al., 2025; Shah et al., 2025).

Despite the remarkable capabilities of RL-trained LLMs, the underlying mechanisms driving their enhancement remain unclear and motivate active debate among the research community. Some studies (Liu et al., 2025; Yue et al., 2025; Shah et al., 2025) examine whether reinforcement learning creates new reasoning solutions from scratch or merely applies existing patterns in base models. Others (Wang et al., 2025; Zhao et al., 2025) demonstrate that the reasoning capability of RL-trained LLMs varies among base model families, motivating more investigation into which base model is best suited for boosting RL's reasoning capabilities. While prior research has not reached a consensus on whether reinforcement learning truly expands the reasoning boundaries of base LLMs, these studies acknowledge that the efficacy of RL is significantly dependent on the initial capabilities of the base model.

Building on the above research consensus, this work seeks to further explore what base model is suitable for RL from the perspective of pre-training dataset mixture strategies. Our focus on the pre-training data mixture stems from prior studies demonstrating its significant impact on base model capabilities (Liu et al., 2024; Xie et al., 2023; Ye et al., 2024b) and subsequently on RL performance (Wang et al., 2025; Zhao et al., 2025). Another issue we need to address is how to choose a suitable base model for RL. There are no straightforward evaluation metrics, such as loss functions, due to the two phases of pre-training and RL training, as well as the complex and unstable RL process (Rafailov et al., 2023; Shao et al., 2024). Inspired by the $\text{pass}@k$ metrics, which are prevailing adopted for evaluating RL-trained LLMs (Liu et al., 2025), we propose to utilize the average perplexity of the base LLM on the RL-generated k responses to evaluate reasoning boundaries of the base model. Such evaluation is agnostic to the specific RL algorithm utilized and may be adapted to any variety (e.g., offline algorithm GPO and online algorithm GRPO), enhancing its versatility.

In summary, we propose an RL algorithm-agnostic method, Go4RL, which first defines the measurement of base models' reasoning capability boundaries as the average perplexity scores of the base LLM on the RL-generated k responses, denoted by $\text{avg}(k\text{-ppl})$. Then Go4RL formulates finding the optimal pre-training dataset mixing ratios for downstream RL as a regression task (Liu et al., 2024), using the proposed $\text{avg}(k\text{-ppl})$ as the fitting objective. Finally, we use the fitted regression model to predict the performance of unseen mixtures and apply the best predicted mixture to train a large-scale model that achieves better RL performance.

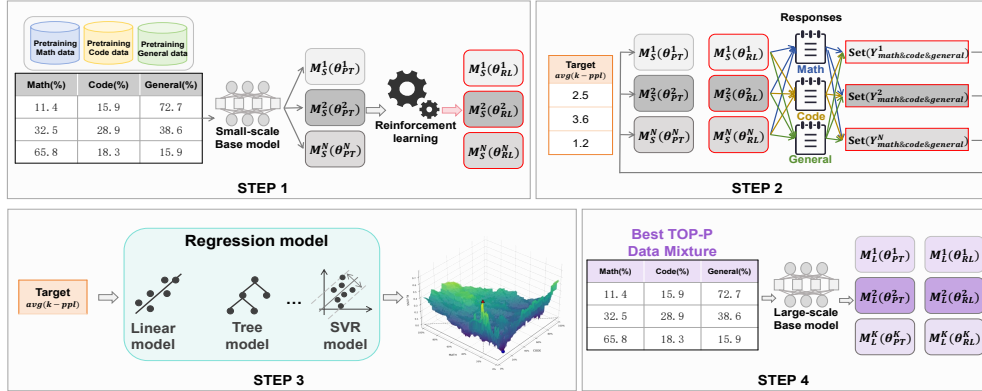
To validate Go4RL, we follow Liu et al. (2024) to train proxy models (both pre-trained and RL-trained) with 1M parameters and scale up to 1B parameters using different data mixtures from three domains (general corpus, math, and coding). Each base model is fine-tuned using RL algorithms directly without supervised fine-tuning. The experimental results on both representative online (GRPO (Shao et al., 2024)) and offline (DPO (Rafailov et al., 2023)) RL algorithms show that the optimized data mixture predicted by Go4RL yields a better base model for RL training.

2 RELATED WORKS

The relationship between the RL and base model. The success of RL-trained LLMs inspires research interest in exploring their underlying mechanism. Existing studies (Yue et al., 2025; Dang et al., 2025; Zhao et al., 2025; Liu et al., 2025) investigate whether reinforcement learning creates new reasoning solutions from scratch or merely applies existing patterns in base models. They suggest that RL-trained models do not gain new reasoning skills beyond those seen in their base models but rather enhance sampling efficiency along right reasoning paths. On the contrary, ProRL (Liu et al., 2025) offers surprising new insights that RL can indeed discover genuinely new solution pathways entirely absent in base models when given sufficient training time and applied to novel reasoning tasks. While the prior research has not reached a consensus on whether RL truly expands the reasoning boundaries of base LLMs, they acknowledge that the efficacy of RL is significantly dependent on the initial capabilities of the base model. Wang et al. (2025) demonstrates that the reasoning capability of RL-trained LLMs varies among base model families, such as Llama (Dubey et al., 2024) and Qwen (Yang et al., 2025). It further proves that the base LLMs could be enhanced for RL through mid-training with a proper data mixture. Differently, we explore how to get an RL-friendly base LLM during the pre-training. Zhao et al. (2025) seeks to clarify how the composition of pretraining data affects the efficacy of RL fine-tuning using varying proportions of the text and math datasets for pre-training. They focus on analyzing the RL reaction on the pre-training data instead of exploring an optimal pre-training data mixture.

Data mixing. Existing LLMs require a huge amount of training data from different data sources to achieve remarkable capabilities. It has been proved that the data mixing strategies have a great impact on the LLMs' performance (Albalak et al., 2023; 2024). As the field progressed, learnable task-performance-driven mixing methods have gradually gained popularity (Schioppa et al., 2023). Task-specific mixing methods generally fall into two categories: offline approaches determine domain weights through proxy model evaluation (Ye et al., 2024b; Liu et al., 2024), while online methods dynamically adjust weights based on feedback during the target model's training (Chen et al., 2023; Xie et al., 2023; Fan et al., 2023). Notably, recent works have leveraged scaling laws or regression models to provide guidance for forecasting data mixing performance in large-scale models (Hoffmann et al., 2022; Muennighoff et al., 2023; Liu et al., 2024). We choose the regression

108 model (Liu et al., 2024) over the scaling law (Ye et al., 2024a) to forecast appropriate data mixture
 109 ratios for large-scale LLMs due to a lack of straightforward evaluation metrics for our problem. Our
 110 work has a different fitting target with Liu et al. (2024).



111
 112
 113
 114
 115
 116
 117
 118
 119
 120
 121
 122
 123
 124
 125
 126
 127
 128
 129
 130
 131
 132
 133
 134
 135
 136
 137
 138
 139
 140
 141
 142
 143
 144
 145
 146
 147
 148
 149
 150
 151
 152
 153
 154
 155
 156
 157
 158
 159
 160
 161
 Figure 1: The framework of Go4RL, including the following steps: 1) Generate random pre-training data mixtures of math, code, and general domains, then pre-train a series of small-scale proxy models based on these mixtures and continually train these proxy models through reinforcement learning. 2) Obtain the target average perplexity $\text{avg}(k-\text{ppl})$ of the pre-trained model over k responses generated by the RL-trained model. 3) Fit a regression model using the ratios of mixtures and the $\text{avg}(k-\text{ppl})$ as the target label. 4) Leverage the fitted regression model to predict the best mixture for the target value on a large-scale model and further validate the prediction.

3 METHODOLOGY

3.1 OVERVIEW

The scenario in this paper is to identify the optimal pre-training data mixture ratio that yields the best-performing LLM after both pre-training and reinforcement learning stages. As illustrated in Figure 1, the proposed Go4RL involves the following four key steps. **(1)** We first train small proxy models, which will be used later for regression. These small proxy models include both pre-trained and RL-trained models. The pre-trained models are trained using numerous different data mixtures from three domains (general corpus, code, and math). It should be noted that our proposed framework is easy to scale to more domains. The RL-trained models are directly trained from the pre-trained ones. These settings follow the SOTA reasoning model DeepSeek R1 (Guo et al., 2025), which applied RL directly to the base pre-trained LLMs, bypassing any intermediate supervised tuning. The data mixture domains are also predominantly adopted by open-source LLM families such as Llama (Dubey et al., 2024) and QWen (Yang et al., 2025). **(2)** With the small proxy pre-trained and RL-trained models, we calculate the average perplexity scores of pre-trained models on k responses generated by RL-trained models, regarded as $\text{avg}(k-\text{ppl})$. **(3)** Fit a regression model using the data mixture ratios as features and the $\text{avg}(k-\text{ppl})$ calculated in step 2 as the target label of the regression. **(4)** We use the fitted regression model to predict the optimal data mixture on large-scale LLMs and then train models to validate. Next, we will elaborate on the specific details of each step.

3.2 TRAIN SMALL-SCALE PROXY MODELS WITH RANDOM DATA MIXTURES

First, we adopt numerous diverse data mixtures to obtain a series of small-scale proxy models, including both the pre-trained base models and RL-trained models. The mixing ratios are sampled based on a token-distribution-based Dirichlet distribution, ensuring broad coverage of weight extremes while preventing overemphasis on low-frequency token domains.

Specifically, leveraging the Dirichlet distribution (Minka, 2000), we randomly generate N different data mixture ratios across three training domains (math, code, and general) to construct a wide

162 spectrum of sparse and near-uniform distributions:
 163

$$\begin{aligned} 164 \quad Set(R) &= [R^1, R^2, \dots, R^n, \dots, R^N] \\ 165 \quad R^n &= [r_{\text{general}}^n : r_{\text{code}}^n : r_{\text{math}}^n] \end{aligned} \quad (1)$$

167 $R^n \in Set(R)$ denotes the possible pre-training data mixture ratio of three domains (e.g., $R^n = [6 : 2 : 2]$).
 168

169 A set of N small-scale proxy pre-trained models $Set(M_S(\theta_{PT}))$ could be obtained, with each M_S
 170 pre-trained by adopting each data mixture strategy $R^n \in Set(R)$:
 171

$$173 \quad Set(M_S(\theta_{PT})) = [M_S^1(\theta_{PT}^1), M_S^2(\theta_{PT}^2), \dots, M_S^N(\theta_{PT}^N)] \quad (2) \\ 174$$

175 With $Set(M_S(\theta_{PT}))$, we then directly apply reinforcement learning with the same setting to train
 176 each pre-trained proxy model, ultimately obtaining a series of RL-optimized small proxy models:
 177

$$178 \quad Set(M_S(\theta_{RL})) = [M_S^1(\theta_{RL}^1), M_S^2(\theta_{RL}^2), \dots, M_S^N(\theta_{RL}^N)] \quad (3) \\ 179$$

180 3.3 CALCULATE THE AVERAGE PERPLEXITY AVG (K-PPL)

181 The pipeline for RL-trained LLMs consists of two phases: pre-training and RL training. Furthermore,
 182 RL is a sophisticated and unstable approach that has multiple variations, including both online
 183 and offline algorithms with distinct techniques such as DPO (Rafailov et al., 2023) and GRPO (Shao
 184 et al., 2024). As a result, there are no straightforward evaluation metrics for analyzing the data mix-
 185 ture effect on RL-trained models via base models, like the predict-next-token loss function used to
 186 evaluate base LLM data mixing.
 187

188 Inspired by the pass@k metrics, which are widely used to evaluate RL-trained LLMs (Guo et al.,
 189 2025; Liu et al., 2025; Zhao et al., 2025), we propose using the average perplexity of the base LLM
 190 on the RL-generated k responses to assess the base models' reasoning ability boundaries, named
 191 avg(k-ppl). Such avg(k-ppl) evaluation is agnostic to the specific RL algorithm utilized and may
 192 be adapted to any variety (e.g., offline algorithm DPO and online algorithm GRPO), enhancing its
 193 versatility.

194 Generally, given a base proxy model $M_S^n(\theta_{PT}^n)$, its corresponding RL-trained proxy model
 195 $M_S^n(\theta_{RL}^n)$, an input x , and a response $Y = (y_1, y_2, \dots, y_T)$ that is generated by the $M_S^n(\theta_{RL}^n)$,
 196 the perplexity of the pre-trained model for Y is defined as the exponentiated average negative log-
 197 likelihood of a sequence:
 198

$$\begin{aligned} 199 \quad &PPL_{M_S^n(\theta_{PT}^n)}(Y|x) \\ 200 \quad &= \exp\left(-\frac{1}{T} \sum_{t=1}^T \log P(y_T|(x, y_1, \dots, y_{T-1}))\right) \end{aligned} \quad (4)$$

202 Eq.4 reflects the model's ability to predict the given response Y conditioned on the prompt x . Lower
 203 perplexity indicates that the model has a higher likelihood of generating this response.
 204

205 We randomly sample a set of prompts in three domains: $x \in X = [Set(X_{\text{code}}), Set(X_{\text{math}}), Set(X_{\text{general}})]$. Similar to the pass@k (Liu et al., 2025) metrics
 206 for evaluating RL performance, we use each $M_S^n(\theta_{RL}^n)$ to generate k multi-responses for each
 207 prompt x . The set of all these responses is denoted as $Set_{RL}^n(Y)$. Let $\overline{k - ppl}_{PT}^n(Y_{RL})$ be
 208 $M_S^n(\theta_{PT}^n)$'s average perplexity of these responses generated by $M_S^n(\theta_{RL}^n)$, defined as below:
 209

$$\begin{aligned} 212 \quad \overline{k - ppl}_{PT}^n(Y_{RL}) &= \frac{\sum_{Y_\alpha \in Set_{RL}^n(Y)} PPL_{M_S^n(\theta_{PT}^n)}(Y_\alpha|x_\alpha)}{l_1 + l_2 + l_3} \\ 213 \quad PPL_{M_S} &= [\overline{k - ppl}_{PT}^1(Y_{RL}), \dots, \overline{k - ppl}_{PT}^N(Y_{RL})] \\ 214 \quad Set_{RL}^n(Y) &= Set(Y_{\text{code}}^{l_1}) \cup Set(Y_{\text{math}}^{l_2}) \cup Set(Y_{\text{general}}^{l_3}) \end{aligned} \quad (5)$$

216 Where l_1, l_2, l_3 respectively represent the number of $M_S^n(\theta_{RL}^n)$'s responses in three domains. Y_α
 217 denotes each response in $Set_{RL}^n(Y)$, while x_α is its corresponding prompt.
 218

219 The definition of avg(k-ppl) can effectively evaluate the reasoning capabilities boundaries of pre-
 220 trained models (Liu et al., 2025). Once we have obtained these avg(k-ppl), we can use the data
 221 mixture as features and the avg(k-ppl) as target labels to fit a regression model.

222 **3.4 FIT A REGRESSION MODEL USING THE DATA MIXTURES AS FEATURES AND THE**
 223 **AVG(K-PPL) AS THE TARGET LABEL**
 224

225 The next step is to fit a regression model using the data mixture ratios of three domains as features
 226 and the avg(k-ppl) as target labels. We choose the regression model (Liu et al., 2024) over the
 227 scaling law (Ye et al., 2024a) to forecast appropriate data mixture ratios for large-scale LLMs due
 228 to a lack of straightforward evaluation metrics for our problem. With the regression model, we are
 229 able to leverage a limited set of small models to estimate continuous target values for unknown data
 230 mixture ratios.

231 Specifically, considering the input features correspond to the domain ratios of the data mixture
 232 $R^n = [r_{general}^n : r_{code}^n : r_{math}^n]$, and the target label $\overline{k - ppl}_{PT}^n(Y_{RL}) \in PPL_{MS}$, the goal is to
 233 find a function that best maps the input features to the target variable.

234 Taking linear regression as an example, which assumes a linear relationship between the input fea-
 235 tures and the target variable, can be represented as:

$$\overline{k - ppl}_{PT}^n(Y_{RL}) = \omega_0 + \omega_1 r_{general}^n + \omega_2 r_{code}^n + \omega_3 r_{math}^n \quad (6)$$

236 Where ω_0 represents the error or noise in the data, and $\omega = (\omega_1, \omega_2, \omega_3)$ are the coefficients asso-
 237 ciated with the respective input features $(r_{general}^n : r_{code}^n : r_{math}^n)$. The coefficients ω are typically
 238 estimated using techniques such as ordinary least squares, aiming to minimize the sum of squared
 239 residuals between the predicted and actual target values.

240 Alternative regression algorithms such as LightGBM (Ke et al., 2017) or SVR (Brereton & Lloyd,
 241 2010) can also be used for fitting the regression models. Using known training data mixtures, these
 242 regression models can learn a predictive function that can estimate target values for arbitrary data
 243 mixtures without requiring additional training.

244 Once the regression model is fitted, we can efficiently explore the entire space of possible data
 245 mixtures. By leveraging the regression model to predict target values for each potential mixture, we
 246 rapidly identify the optimal input features $R^{best} = [r_{general}^{best} : r_{code}^{best} : r_{math}^{best}]$ that yield the lowest
 247 $\overline{k - ppl}_{PT}^n(Y_{RL})$ within an infinite set PPL_{MS} :

$$[r_{general}^{best} : r_{code}^{best} : r_{math}^{best}] = \underset{R^n \in Set(R)}{\operatorname{argmin}} (\overline{k - ppl}_{PT}^n(Y_{RL})) \quad (7)$$

248 This simulation-based optimization significantly reduces costs, as both small-scale model simula-
 249 tions and regression predictions are computationally inexpensive.

250 **3.5 TRAIN LARGE-SCALE MODELS USING THE PREDICTED OPTIMAL DATA MIXTURE**
 251

252 After simulating and predicting the optimal data mixtures via the regression model, we apply the
 253 predicted top-P mixture ratios to sample large-scale pre-training data:

$$Set(R^{topP}) = [R_{top}^1, \dots, R_{top}^P] \quad (8)$$

254 According to the hypothesis proposed and proved by Liu et al. (2024), the rank invariance of data
 255 mixtures posits that the relative ranking of data mixtures in terms of their impact on model per-
 256 formance remains consistent across different model scales and training token quantities. Thus, we train
 257 a larger model using these optimally mixed data, going through both pre-training and RL phases:

$$\begin{aligned} Set(M_L^{topP}(\theta_{PT})) &= [M_L^1(\theta_{PT}^1), \dots, M_L^P(\theta_{PT}^P)] \\ Set(M_L^{topP}(\theta_{RL})) &= [M_L^1(\theta_{RL}^1), \dots, M_L^P(\theta_{RL}^P)] \end{aligned} \quad (9)$$

258 We can subsequently employ these well-trained larger models to perform the corresponding down-
 259 stream tasks.

270 4 EXPERIMENTS
271272 4.1 EXPERIMENTAL SETUPS
273274 **Datasets and benchmarks.** For the pre-training stage, we train on a mixture of three datasets
275 for code, math, and general corpus separately: TheStack (Kocetkov et al., 2022), OpenWebMath
276 (Paster et al., 2023), and the subset C4 dataset of redpajama (Together, 2023). During the reinforce-
277 ment learning fine-tuning phase, we train on instruction datasets such as python-code-25k (FlyTech,
278 2024), OMNI-MATH (Gao et al., 2024) and GSM8K (Cobbe et al., 2021) to further optimize the
279 model. Then, we choose the following representative downstream benchmarks used by LLMs to
280 assess the model’s broad generalization capacity. General tasks: OpenBookQA(OBQA)(Mihaylov
281 et al., 2018), PIQA(Bisk et al., 2020) and Hellaswag(Zellers et al., 2019). Coding tasks: HumanEval
282 (Chen et al., 2021) and MBPP (Austin et al., 2021). Math tasks: MATH (Hendrycks et al., 2021)
283 and GSM8K (Cobbe et al., 2021). The adoption of these datasets and benchmarks is aligned with
284 the publicly released LLMs’ technical reports (Dubey et al., 2024; M-A-P, 2024; Guo et al., 2025).
285286 **Metrics.** For the regression model, we follow Liu et al. (2024) and employ two metrics to eval-
287 uate the regression model: the Spearman rank correlation coefficient (ρ) and mean squared error
288 (MSE). The Spearman correlation ρ provides a nonparametric measure of the strength and direction
289 of association between two variables, while MSE evaluates the regression model’s performance for
290 small-scale proxy models by measuring the average squared difference between predicted and ac-
291 tual values. For the RL-trained LLMs, each downstream task is evaluated using its corresponding
292 standard evaluation metrics.293 **Baselines.** We compare Go4RL with four baselines: *Human*, *PPL*, *RL-loss*, and *Worst*. *Human*
294 employs manual ratio allocation for data across the three domains based on empirical training ex-
295 perience according to the release of LLMs’ technical reports (Dubey et al., 2024; M-A-P, 2024).
296 Specifically, the mixing ratio for code, math, and general is 0.33:0.15:0.52. *PPL* uses the perplex-
297 ity filtering methods from Ankner et al. (2024), selecting pretraining data by evaluating the model’s
298 perplexity on candidate data samples. *RL-loss* replaces the regression model’s fitting target of $\text{avg}(k\text{-ppl})$
299 with the loss of the RL phase. *Worst* uses top-5 worst data mixtures selected by Go4RL.300 **Implementation details.** For small-scale proxy models, we train a total number of 512 Transformer-
301 based decoder-only language models with 1M parameters for 1B tokens, calculating their $\text{avg}(k\text{-ppl})$
302 scores to fit a regression model. We then validate the regression model on 256 unseen data mixtures
303 across pretrained language models with 1M, 60M, and 1B parameters. Finally, we train and evaluate
304 the 1B-parameter model on 64 unseen data mixtures with a total of 25B tokens. Following the
305 methodology of Liu et al. (2024), we scale the token distribution by values ranging from 0.1 to 5.0
306 to construct a wide spectrum of sparse and near-uniform distributions. These scaled distribution
307 vectors are then used as the hyperparameters α for the Dirichlet sampling. We consider LightGBM,
308 ridge regression, and random forest as our regression models.309 We pre-train the decoder-only base models with 1 epoch, using the Adam optimizer in a batch size of
310 128K with a learning rate of 4e-4. The weight decay is 0.005. For the reinforcement learning stage,
311 we employ both representative online (GRPO (Shao et al., 2024) following Deepseek-r1 (Guo et al.,
312 2025)) and offline (DPO (Rafailov et al., 2023)) RL algorithms. Due to space constraints, the main
313 text presents part of the experimental results, while the other experimental results are provided in
314 the Appendix. We guide the learning of the model by quantifying the quality of its answers, scoring
315 based on the output format and the final answer. k responses for calculating the $\text{avg}(k\text{-ppl})$ is set to
316 8. Our setup consists of a four-core CPU and eight NVIDIA Tesla A100 GPUs.317 4.2 THE PERFORMANCE OF THE REGRESSION MODEL
318319 We first evaluate the ability of the regression model, including the fitting results over different re-
320 gression algorithms, and the performance in predicting the effect of unseen data mixtures.321 **(1) Fitting results over different regression algorithms.** We fit the regression model using small
322 proxy models with 1M parameters and evaluate the loss prediction performance on small models
323 with the same parameters. As illustrated in Table 1, we adopt three representative regression al-
324 gorithms: Light GBM, Ridge Regression, and Random Forest. LightGBM surpasses the other two

324 regression methods in predicting the unseen data mixing ratio over the same 1M parameter models,
 325 achieving 86.46% in the ρ metric and 0.34 in the MSE metric.
 326

327 Table 1: We separately fit three regression models based on the results of the 1M parameter models
 328 trained on 1B tokens and validate them on unseen data mixtures for 1M, 60M, and 1B parameter
 329 models. The 60M parameter model is trained with 1B tokens, while the 1B model is trained with
 330 25B tokens. ρ compares the predicted and actual data mixtures, while MSE measures the differences
 331 between the target performances of the predicted and actual models.

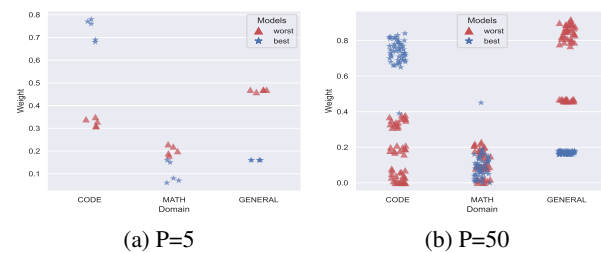
Model Size	1M		60M	1B
Metrics	ρ	MSE	ρ	ρ
LightGBM	86.46	0.34	69.12	58.33
Ridge Regression	83.12	0.37	61.65	51.67
Random Forest	73.24	0.45	38.8	8.33

332
 333 The regression models are then used to predict models with scaled-up parameters and tokens. The
 334 prediction for larger models with more tokens demonstrates that regression models trained on small
 335 proxy models can be applied to larger-scale models. We train different 60M and 1B parameter LLM
 336 models (both pre-trained and RL-trained) to evaluate the deviation between the predicted and actual
 337 results for unseen data mixtures.

338 Table 1 shows that the regression models of LightGBM and Ridge Regression performed reason-
 339 ably well across all three model scales. The random forest method fails to predict scaled-up models,
 340 which may be because the tree-structure-based algorithm could not learn the complex internal pat-
 341 tern of the pre-training and RL-training pipeline. While prediction accuracy declined as model size
 342 increased for all three regression models, the Spearman rank correlation consistently remain around
 343 70% and 60% for LightGBM. The variance in prediction performance of parameter-scaled models
 344 may be attributed to shifts in data samples from a single data source, particularly the training tokens
 345 scaled for larger models, e.g., 25b tokens for 1B parameter models. Among these, LightGBM ex-
 346 hibits the most outstanding performance, outperforming the RidgeRegression by around 8% points.
 347 These results validate the feasibility of the rank-invariance-based approach for predicting optimal
 348 data mixtures.

349 **(2) Deep analysis of the fitted LightGBM performance on predicting the data mixture.** To fur-
 350 ther analyze the distribution of the top-P mixtures, we separately visualize their weight distributions
 351 across all three domains (general, code, and math). As shown in Figure 2(b) with P=50, we observe
 352 that top-ranked data mixtures consistently contained a higher proportion of domain code up to the
 353 range of 70% to 80%, while the proportion of general text stays close to 20%. This phenomenon
 354 aligns with the findings reported in Zhao et al. (2025)'s study.

361 4.3 THE IMPACT OF PREDICTED MIXTURE ON DOWNSTREAM TASKS



362 Figure 2: The distribution of Top-P (P=5, 50) best and
 363 worst mixtures across three domains.

364
 365 We validate the efficacy of Go4RL
 366 on downstream reasoning tasks. The
 367 selected benchmarks are prevalently
 368 adopted by released LLMs (Dubey
 369 et al., 2024; Guo et al., 2025) and
 370 comprehensively cover tasks across three
 371 domains: code, mathematics, and gen-
 372 eral reasoning, enabling a holistic eval-
 373 uation of Go4RL's capabilities. We com-
 374 pare the Go4RL predicted data mix-
 375 ture with four baselines: HUMAN, PPL,
 376 Worst, and RL_loss. Refer to the
 377 details of these baselines in experimental
 378 setups. We first utilize Go4RL to pre-
 379 dict the top 5 best and worst data mix-
 380 ture strategies. We train 1B parameter base
 381 models using both GRPO and DPO to get RL-trained models separately.

Table 2 lists the average performance of 1B models trained by GRPO, using the top-5 best data mixtures selected by Go4RL. The results with DPO are listed in the Table 5 in appendix due to the page limit. According to Table 2, pretraining data mixtures using the proposed optimization objective $\text{avg}(k\text{-ppl})$ have an obvious impact on reasoning downstream tasks. Compared to the four baselines, Go4RL demonstrates a superior performance, outperforming all four competing baselines in 4 out of 7 tasks while achieving the highest average score (3.8% higher than RL_loss). The average performance improvement across all the tasks highlights both the crucial role of data mixtures in the pretraining+RL pipeline and the validity of our data selection method. Note that the RL_loss baseline shows suboptimal performance, indicating that the RL loss function alone is not an adequate metric for the pre-train+RL pipeline. We also notice the performance decline on GSM8K . The potential reason may be its data format deviating significantly from the training data OpenWebMath . Similar phenomena have been found in other works (Zhao et al., 2025). Besides, the settings of our RL stage comprise GSM8K training data. The performance decay may reflect prior research of the RL narrowing the reasoning bounds of the base model (Yue et al., 2025). This also indicates the complexity of the relationship between pre-training and RL, which needs further exploration.

Table 2: Average performance of 1B models trained by GRPO, using the top-5 best data mixtures selected by Go4RL, compared with several other data selection baselines. BSET ON indicates how many of all tasks the model achieves the best results in. The reported performance on each task is the average score of 3 runs, while the highest score on each task is highlighted in bold.

	Domain	General			Code		Math		Avg.	Best On
		Tasks	OBQA	PIQA	Hellaswag	Humaneval	MBPP	MATH		
Baselines	Metrics	Acc.	Acc.	Acc.	Pass@10	Pass@10	Acc	Acc		
	HUMAN	17.8	14.3	22.9	7.3	0.6	0.4	0.5	9.1	0
	PPL	18.8	17.2	24.6	9.2	1.4	0.6	2.8	10.7	2
Go4RL	RL_loss	5.8	24.5	23.0	20.1	6.0	0.9	1.9	11.7	1
	Worst	18.5	16.7	25.1	16.9	2.7	0.6	0.3	11.5	0
	Best	12.5	21.2	25.3	36.8	10.5	1.1	0.9	15.5	4

We further plot the top-5 best data mixture ratio distributions as illustrated in Figure 2(a). The best data mixture strategies have a relatively high ratio on the code domain and a similar low ratio on both the general and math domains. However, the downstream tasks show performance gain over all the domains.

4.4 HOW DOES THE PERFORMANCE OF MODELS WITH DIFFERENT DATA MIXTURES IMPROVE DURING RL?

We are interested in how the RL-trained models favor the domain distribution with the accumulated RL steps. As shown in Figure 3, we compare trajectories during RL of the models pretrained with data mixtures selected by Go4RL (top-5 best) with the random sampling, Go4RL-worst, and RL_loss under the DPO algorithm. For the code domain, we compare the pass@k ($k=1,10$) trajectories over MPBB and Humaneval. Go4RL-best demonstrates strong RL gains from the starting point on Humaneval, eventually achieving the largest RL reasoning gains for both the pass@1 and pass@10 evaluations on all the Code tasks. For both MATH and GSM8K , Go4RL-best demonstrates a clear advantage during RL. It can be observed that the uptrend of the RL gains for the MPBB and MATH benchmarks with the Go4RL-optimized data mixture. For many benchmarks, we noticed that the RL_loss baseline displays initial performance gains while fluctuating as the RL steps accumulate. These results further reflect the recent findings of the entropy collapse phenomenon for RL phase (Yu et al., 2025). It also proves that the performance in the RL phase is not the sole factor affecting downstream knowledge expression and generation, finding a suitable base model also plays a significant role. The results with GRPO are listed in Figure 7 in the Appendix.

4.5 WHAT'S A PROPER MEASUREMENT FOR THE DATA MIXTURES TARGETING RL PERFORMANCE?

We want to further check if the proposed $\text{avg}(k\text{-ppl})$ is proper for the performance measurements by evaluating its correlation with the data mixture ratios. It should be noted that there are other options, such as the downstream task accuracy and RL loss. RL loss has been proven to be inadequate in the

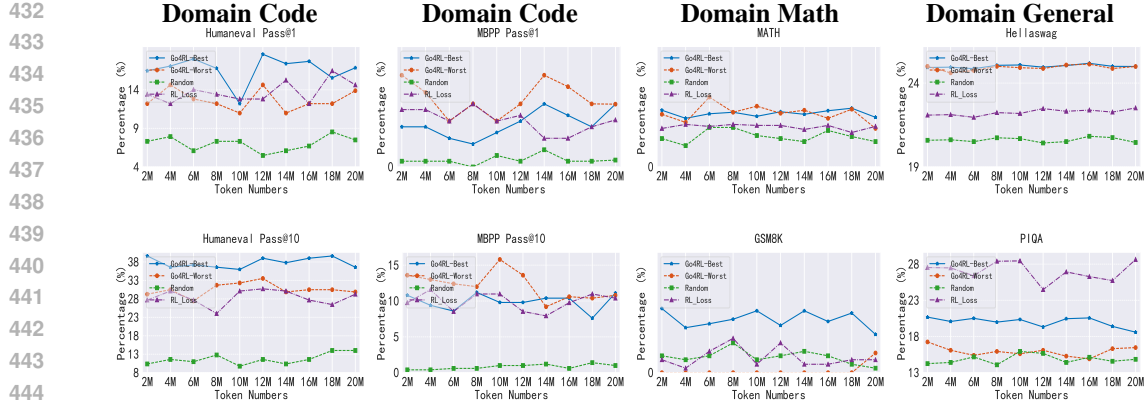


Figure 3: Three domains’ downstream performances of the Go4RL-optimal 1B parameter models (RL-trained with DPO) with top-5 best data mixtures, compared with the random sampling, RL_loss and Go4RL selected worst baselines. The x-axis is the growing training tokens in the RL stage.

previous analysis. We visualize the correlation between the avg(k-ppl), the potential measurement of downstream task accuracy, and the different data domains under the GRPO.

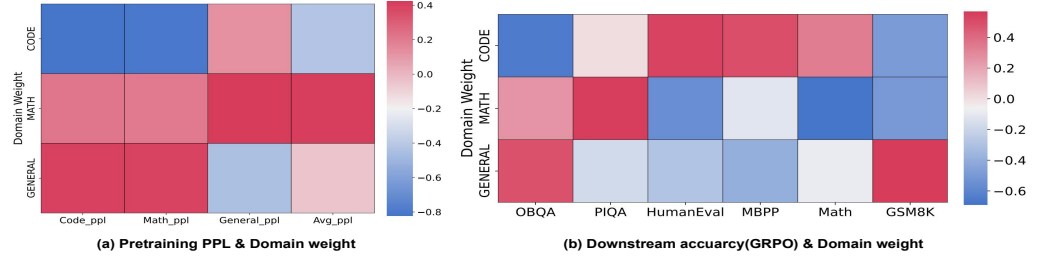


Figure 4: (a) The correlations between avg(k-ppl) and training data ratios across three domains separately and averaged over 1B models. (b) The correlations between downstream accuracy and training domain ratios on 1B models.

According to Figure 4(a), illustrating the correlation during pre-training stages, the avg(k-ppl) elaborates a high correlation with the data domain ratios, demonstrating its effectiveness in evaluating a suitable base model for RL. In the pre-training stage, data from the math domain provides gains to all other domains. The general domain significantly influences both code_ppl and math_ppl, which are calculated as the avg(k-ppl) from the code and math domains separately. For the downstream tasks illustrated in Figure 4(b), the data from the code source exhibits a pronounced negative impact on OBQA, which gives an explanation of the OBQA performance decline and performance of code benchmarks increase in Table 2. The visualization results highlight the importance and inherent complexity of determining the optimal pre-training data mixture and give hints for the further improvement of the Go4RL method.

5 CONCLUSION

On the basis of the recent research findings, we propose a framework Go4RL, to predict optimal data mixture strategies that effectively make the base model suitable for augmenting RL’s reasoning capabilities. Leveraging the ratios of data from different domains as features and the proposed average perplexity of the responses generated by the RL-trained models as the target, Go4RL fits a regression model to predict the optimal data mixture leading to enhanced RL capabilities. We conduct experiments to validate Go4RL’s performance. Our work gives a first insight into how the pre-trained data mixture of the base model further impacts the RL models that could potentially inspire broad discussion in the research community.

486 REFERENCES
487

488 Josh Achiam, Steven Adler, Sandhini Agarwal, Lama Ahmad, Ilge Akkaya, Florencia Leoni Ale-
489 man, Diogo Almeida, Janko Altenschmidt, Sam Altman, Shyamal Anadkat, et al. Gpt-4 technical
490 report. *arXiv preprint arXiv:2303.08774*, 2023.

491 Alon Albalak, Liangming Pan, Colin Raffel, and William Yang Wang. Efficient online data mixing
492 for language model pre-training. *arXiv preprint arXiv:2312.02406*, 2023.

493

494 Alon Albalak, Yanai Elazar, Sang Michael Xie, Shayne Longpre, Nathan Lambert, Xinyi Wang,
495 Niklas Muennighoff, Bairu Hou, Liangming Pan, Haewon Jeong, et al. A survey on data selection
496 for language models. *arXiv preprint arXiv:2402.16827*, 2024.

497 Zachary Ankner, Cody Blakeney, Kartik Sreenivasan, Max Marion, Matthew L Leavitt, and Man-
498 sheej Paul. Perplexed by perplexity: Perplexity-based data pruning with small reference models.
499 *arXiv preprint arXiv:2405.20541*, 2024.

500

501 Jacob Austin, Augustus Odena, Maxwell Nye, Maarten Bosma, Henryk Michalewski, David Dohan,
502 Ellen Jiang, Carrie Cai, Michael Terry, Quoc Le, et al. Program synthesis with large language
503 models. *arXiv preprint arXiv:2108.07732*, 2021.

504

505 Yonatan Bisk, Rowan Zellers, Jianfeng Gao, Yejin Choi, et al. Pixa: Reasoning about physical com-
506 monsense in natural language. In *Proceedings of the AAAI conference on artificial intelligence*,
507 volume 34, pp. 7432–7439, 2020.

508 Richard G Brereton and Gavin R Lloyd. Support vector machines for classification and regression.
509 *Analyst*, 135(2):230–267, 2010.

510

511 Mark Chen, Jerry Tworek, Heewoo Jun, Qiming Yuan, Henrique Ponde De Oliveira Pinto, Jared
512 Kaplan, Harri Edwards, Yuri Burda, Nicholas Joseph, Greg Brockman, et al. Evaluating large
513 language models trained on code. *arXiv preprint arXiv:2107.03374*, 2021.

514

515 Mayee Chen, Nicholas Roberts, Kush Bhatia, Jue Wang, Ce Zhang, Frederic Sala, and Christopher
516 Ré. Skill-it! a data-driven skills framework for understanding and training language models.
517 *Advances in Neural Information Processing Systems*, 36:36000–36040, 2023.

518

519 Karl Cobbe, Vineet Kosaraju, Mohammad Bavarian, Mark Chen, Heewoo Jun, Lukasz Kaiser,
520 Matthias Plappert, Jerry Tworek, Jacob Hilton, Reiichiro Nakano, et al. Training verifiers to
521 solve math word problems. *arXiv preprint arXiv:2110.14168*, 2021.

522

523 Xingyu Dang, Christina Baek, J Zico Kolter, and Aditi Raghunathan. Assessing diversity collapse
524 in reasoning. In *Scaling Self-Improving Foundation Models without Human Supervision*, 2025.

525

526 Abhimanyu Dubey, Abhinav Jauhri, Abhinav Pandey, Abhishek Kadian, Ahmad Al-Dahle, Aiesha
527 Letman, Akhil Mathur, Alan Schelten, Amy Yang, Angela Fan, et al. The llama 3 herd of models.
528 *arXiv e-prints*, pp. arXiv–2407, 2024.

529

530 Simin Fan, Matteo Pagliardini, and Martin Jaggi. Doge: Domain reweighting with generalization
531 estimation. *arXiv preprint arXiv:2310.15393*, 2023.

532

533 FlyTech. flytech/python-codes-25k, 2024. URL <https://huggingface.co/datasets/flytech/python-codes-25k>.

534

535 Bofei Gao, Feifan Song, Zhe Yang, Zefan Cai, Yibo Miao, Qingxiu Dong, Lei Li, Chenghao Ma,
536 Liang Chen, Runxin Xu, Zhengyang Tang, Benyou Wang, Daoguang Zan, Shanghaoran Quan,
537 Ge Zhang, Lei Sha, Yichang Zhang, Xuancheng Ren, Tianyu Liu, and Baobao Chang. Omni-
538 math: A universal olympiad level mathematic benchmark for large language models, 2024. URL
539 <https://arxiv.org/abs/2410.07985>.

540

541 Daya Guo, Dejian Yang, Haowei Zhang, Junxiao Song, Ruoyu Zhang, Runxin Xu, Qihao Zhu,
542 Shirong Ma, Peiyi Wang, Xiao Bi, et al. Deepseek-r1: Incentivizing reasoning capability in llms
543 via reinforcement learning. *arXiv preprint arXiv:2501.12948*, 2025.

540 Dan Hendrycks, Collin Burns, Saurav Kadavath, Akul Arora, Steven Basart, Eric Tang, Dawn Song,
 541 and Jacob Steinhardt. Measuring mathematical problem solving with the math dataset. *arXiv*
 542 *preprint arXiv:2103.03874*, 2021.

543

544 Jordan Hoffmann, Sebastian Borgeaud, Arthur Mensch, Elena Buchatskaya, Trevor Cai, Eliza
 545 Rutherford, Diego de Las Casas, Lisa Anne Hendricks, Johannes Welbl, Aidan Clark, et al. Training
 546 compute-optimal large language models. *arXiv preprint arXiv:2203.15556*, 2022.

547

548 Aaron Jaech, Adam Kalai, Adam Lerer, Adam Richardson, Ahmed El-Kishky, Aiden Low, Alec
 549 Helyar, Aleksander Madry, Alex Beutel, Alex Carney, et al. Openai o1 system card. *arXiv*
 550 *preprint arXiv:2412.16720*, 2024.

551

552 Guolin Ke, Qi Meng, Thomas Finley, Taifeng Wang, Wei Chen, Weidong Ma, Qiwei Ye, and Tie-
 553 Yan Liu. Lightgbm: A highly efficient gradient boosting decision tree. *Advances in neural*
 554 *information processing systems*, 30, 2017.

555

556 Denis Kocetkov, Raymond Li, Loubna Ben Allal, Jia Li, Chenghao Mou, Carlos Muñoz Ferrandis,
 557 Yacine Jernite, Margaret Mitchell, Sean Hughes, Thomas Wolf, Dzmitry Bahdanau, Leandro von
 558 Werra, and Harm de Vries. The stack: 3 tb of permissively licensed source code. *Preprint*, 2022.

559

560 Mingjie Liu, Shizhe Diao, Ximing Lu, Jian Hu, Xin Dong, Yejin Choi, Jan Kautz, and Yi Dong.
 561 Prorl: Prolonged reinforcement learning expands reasoning boundaries in large language models.
 562 *arXiv preprint arXiv:2505.24864*, 2025.

563

564 Qian Liu, Xiaosen Zheng, Niklas Muennighoff, Guangtao Zeng, Longxu Dou, Tianyu Pang, Jing
 565 Jiang, and Min Lin. Regmix: Data mixture as regression for language model pre-training. *arXiv*
 566 *preprint arXiv:2407.01492*, 2024.

567

568 Wuhan AI Research M-A-P, University of Waterloo. Map-neo: Highly capable and transparent
 569 bilingual large language model serie. <https://map-neo.github.io/>, 2024.

570

571 Todor Mihaylov, Peter Clark, Tushar Khot, and Ashish Sabharwal. Can a suit of armor conduct
 572 electricity? a new dataset for open book question answering. *arXiv preprint arXiv:1809.02789*,
 573 2018.

574

575 Thomas Minka. Estimating a dirichlet distribution, 2000.

576

577 Niklas Muennighoff, Alexander Rush, Boaz Barak, Teven Le Scao, Nouamane Tazi, Aleksandra
 578 Piktus, Sampo Pyysalo, Thomas Wolf, and Colin A Raffel. Scaling data-constrained language
 579 models. *Advances in Neural Information Processing Systems*, 36:50358–50376, 2023.

580

581 Long Ouyang, Jeffrey Wu, Xu Jiang, Diogo Almeida, Carroll Wainwright, Pamela Mishkin, Chong
 582 Zhang, Sandhini Agarwal, Katarina Slama, Alex Ray, et al. Training language models to fol-
 583 low instructions with human feedback. *Advances in neural information processing systems*, 35:
 584 27730–27744, 2022.

585

586 Keiran Paster, Marco Dos Santos, Zhangir Azerbayev, and Jimmy Ba. Openwebmath: An open
 587 dataset of high-quality mathematical web text, 2023.

588

589 Rafael Rafailov, Archit Sharma, Eric Mitchell, Christopher D Manning, Stefano Ermon, and Chelsea
 590 Finn. Direct preference optimization: Your language model is secretly a reward model. *Advances*
 591 *in neural information processing systems*, 36:53728–53741, 2023.

592

593 Andrea Schioppa, Xavier Garcia, and Orhan Firat. Cross-lingual supervision improves large lan-
 594 guage models pre-training. *arXiv preprint arXiv:2305.11778*, 2023.

595

596 Darsh J Shah, Peter Rushton, Somanshu Singla, Mohit Parmar, Kurt Smith, Yash Vanjani, Ashish
 597 Vaswani, Adarsh Chaluvvaraju, Andrew Hojel, Andrew Ma, et al. Rethinking reflection in pre-
 598 training. *arXiv preprint arXiv:2504.04022*, 2025.

599

600 Zhihong Shao, Peiyi Wang, Qihao Zhu, Runxin Xu, Junxiao Song, Xiao Bi, Haowei Zhang,
 601 Mingchuan Zhang, YK Li, Yang Wu, et al. Deepseekmath: Pushing the limits of mathemati-
 602 cal reasoning in open language models. *arXiv preprint arXiv:2402.03300*, 2024.

594 Yunhao Tang, Zhaohan Daniel Guo, Zeyu Zheng, Daniele Calandriello, Rémi Munos, Mark Row-
 595 land, Pierre Harvey Richemond, Michal Valko, Bernardo Ávila Pires, and Bilal Piot. Generalized
 596 preference optimization: A unified approach to offline alignment. *arXiv preprint arXiv:2402.05749*, 2024.
 597

598 AI Together. Redpajama: An open source recipe to reproduce llama training dataset, 2023. URL
 599 <https://github.com/togethercomputer/RedPajama-Data>.
 600

601 Zengzhi Wang, Fan Zhou, Xuefeng Li, and Pengfei Liu. Octothinker: Mid-training incentivizes
 602 reinforcement learning scaling. *arXiv preprint arXiv:2506.20512*, 2025.
 603

604 Sang Michael Xie, Hieu Pham, Xuanyi Dong, Nan Du, Hanxiao Liu, Yifeng Lu, Percy S Liang,
 605 Quoc V Le, Tengyu Ma, and Adams Wei Yu. Doremi: Optimizing data mixtures speeds up
 606 language model pretraining. *Advances in Neural Information Processing Systems*, 36:69798–
 607 69818, 2023.
 608

608 An Yang, Anfeng Li, Baosong Yang, Beichen Zhang, Binyuan Hui, Bo Zheng, Bowen Yu,
 609 Chang Gao, Chengan Huang, Chenxu Lv, et al. Qwen3 technical report. *arXiv preprint arXiv:2505.09388*, 2025.
 610

611 Jiasheng Ye, Peiju Liu, Tianxiang Sun, Jun Zhan, Yunhua Zhou, and Xipeng Qiu. Data mixing
 612 laws: Optimizing data mixtures by predicting language modeling performance. *arXiv preprint arXiv:2403.16952*, 2024a.
 613

614 Jiasheng Ye, Peiju Liu, Tianxiang Sun, Jun Zhan, Yunhua Zhou, and Xipeng Qiu. Data mixing
 615 laws: Optimizing data mixtures by predicting language modeling performance. *arXiv preprint arXiv:2403.16952*, 2024b.
 616

617 Qiying Yu, Zheng Zhang, Ruofei Zhu, Yufeng Yuan, Xiaochen Zuo, Yu Yue, Weinan Dai, Tiantian
 618 Fan, Gaohong Liu, Lingjun Liu, et al. Dapo: An open-source llm reinforcement learning system
 619 at scale. *arXiv preprint arXiv:2503.14476*, 2025.
 620

621 Yang Yue, Zhiqi Chen, Rui Lu, Andrew Zhao, Zhaokai Wang, Shiji Song, and Gao Huang. Does re-
 622inforcement learning really incentivize reasoning capacity in llms beyond the base model? *arXiv preprint arXiv:2504.13837*, 2025.
 623

624 Rowan Zellers, Ari Holtzman, Yonatan Bisk, Ali Farhadi, and Yejin Choi. Hellaswag: Can a ma-
 625chine really finish your sentence? *arXiv preprint arXiv:1905.07830*, 2019.
 626

627 Rosie Zhao, Alexandru Meterez, Sham Kakade, Cengiz Pehlevan, Samy Jelassi, and Eran Malach.
 628 Echo chamber: Rl post-training amplifies behaviors learned in pretraining. *arXiv preprint arXiv:2504.07912*, 2025.
 629

632 A THE USE OF LARGE LANGUAGE MODELS (LLMs) 633

634 We appreciate the assistance provided by GPT-4 (Achiam et al., 2023) in writing aid and sentence-
 635 level polishing.
 636

637 B RL ALGORITHM DETAILS 638

639 B.1 PRELIMINARY 640

641 We model a LLM as a policy $\pi_\theta(y|x)$ parameterized by θ , where π_θ generates a text response $y \in Y$
 642 conditioned on a user instruction $x \in X$. Given a prompt x , the LLM π_θ will generate response y
 643 in an auto-regressive manner:
 644

$$\pi_\theta(y|x) = \prod_t \pi_\theta(y_t|x, y_{<t}) \quad (10)$$

645 where y_t denotes the t -th token in the response, and $y_{<t}$ represents the sequence of tokens preceding
 646 y_t .
 647

648 **RLHF**: To further align the SFT model π_θ with human preferences, prior studies introduce the
 649 Reinforcement Learning from Human Feedback (RLHF) framework (Ouyang et al., 2022), which
 650 optimizes the following objective:
 651

$$652 \quad \mathcal{L}_r(\pi_\theta) = \mathbb{E}_{x \sim p_{data}, y \sim \pi_\theta} [r(x, y) - \beta \log \frac{\pi_\theta(y|x)}{\pi_{ref}(y|x)}] \quad (11)$$

$$653$$

654 where r denotes the reward function that captures human preferences, mapping a prompt–response
 655 pair to a scalar value. π_{ref} is the reference model used to regularize π_θ via Kullback–Leibler diver-
 656 gence, and β is a constant that controls the strength of this regularization.
 657

658 **B.2 DPO**

660 A line of RL works aims to skip the reward modeling step and may be referred to as the direct prefer-
 661 ence learning approach (Tang et al., 2024). Among them, the direct preference optimization (DPO)
 662 algorithm is the most popular one. DPO (Rafailov et al., 2023) is a preference-based alignment
 663 algorithm that directly optimizes the language model toward human-preferred outputs without rely-
 664 ing on reinforcement learning. Instead of training a reward model as in RLHF, DPO reformulates
 665 preference learning as a supervised objective over pairs of responses.
 666

667 Specifically, it leverages pairs of preferred and dispreferred responses and maximizes the log-
 668 likelihood of the preferred output relative to the dispreferred one under the model’s distribution.
 669 Given a prompt x with two candidate responses (y^+, y^-) , where y^+ is preferred over y^- according
 670 to human feedback, DPO optimizes the policy π_θ by maximizing the following objective:
 671

$$672 \quad \mathcal{L}_{DPO}(\theta) = \mathbb{E}_{(x, y^+, y^-)} [\log \sigma(\beta(\log \frac{\pi_\theta(y^+|x)}{\pi_{ref}(y^+|x)} - \log \frac{\pi_\theta(y^-|x)}{\pi_{ref}(y^-|x)}))] \quad (12)$$

$$673$$

674 where π_θ is the policy being optimized, π_{ref} is a frozen reference model, β is a temperature param-
 675 eter controlling the sharpness of preference weighting, and $\sigma(\cdot)$ is the logistic sigmoid function.
 676

677 DPO allows direct optimization of the model distribution with respect to preferences, avoiding the
 678 instability of reinforcement learning while maintaining strong alignment performance.
 679

680 **B.3 GRPO**

681 Group Relative Policy Optimization (GRPO) is a reinforcement learning variant proposed in Shao
 682 et al. (2024). It is designed for fine-tuning large language models (LLMs) in reasoning-heavy tasks,
 683 and aims to reduce computational cost and complexity while maintaining high performance. Unlike
 684 Proximal Policy Optimization (PPO), GRPO removes the need for a separate value function (critic),
 685 instead it estimates the baseline using group-based statistics.
 686

687 Given a prompt x , the old policy $\pi_{\theta_{old}}$ samples a group of G candidate responses $\{y_1, y_2, \dots, y_G\}$.
 688 Each response y_i is evaluated by a reward function $r(x, y_i)$, yielding scores $\{r_1, r_2, \dots, r_G\}$. The
 689 group statistics are then computed as:
 690

$$691 \quad \mu = \frac{1}{G} \sum_{i=1}^G r_i, \sigma = \sqrt{\frac{1}{G} \sum_{i=1}^G (r_i - \mu)^2} \quad (13)$$

$$692$$

$$693$$

694 A normalized group-relative advantage is defined for each response as:
 695

$$696 \quad A_i = \frac{r_i - \mu}{\sigma} \quad (14)$$

$$697$$

$$698$$

699 Let the importance sampling ratio be:
 700

$$701 \quad \rho_i = \frac{\pi_\theta(y_i|x)}{\pi_{\theta_{old}}(y_i|x)} \quad (15)$$

$$702$$

702 The GRPO objective extends the PPO surrogate loss with group-relative advantages and KL regu-
 703 larization to a reference model π_{ref} :

$$705 \mathcal{L}_{GRPO}(\theta) = \mathbb{E}_{(x, y_1, \dots, y_G) \sim \pi_{\theta_{old}}} \left[\frac{1}{G} \sum_{i=1}^G \min(\rho_i A_i, \text{clip}(\rho_i, 1-\varepsilon, 1+\varepsilon) A_i) - \beta D_{KL}(\pi_{\theta}(\cdot|x) || \pi_{ref}(\cdot|x)) \right] \quad (16)$$

708 where ε is the clipping parameter that constrains policy updates, and β controls the strength of KL
 709 regularization.

711 GRPO eliminates the need for an explicit value function, replacing it with group-relative statistics
 712 as the baseline, thereby simplifying optimization while maintaining stability.

714 C DETAILS OF MODELS AND SAMPLES

716 C.1 MODEL DETAILS

718 The structures of the series of models are displayed in Table 3. These models utilize the same
 719 vocabulary as Qwen Yang et al. (2025), with a vocabulary size of 151,936.

721 Model	721 1M	721 60M	721 1B
722 Vocabulary Size	151936	151936	151936
n_{layers}	2	10	22
n_{heads}	8	8	16
$n_{embedding}$	256	768	2048
d_{model}	512	1536	5632

727 Table 3: The model structure from different LLMs.

730 C.2 SAMPLE ANALYSIS

731 In the main paper, we hypothesize that the performance drop on GSM8K may stem from its signifi-
 732 cant deviation in data format compared to the training data, OpenWebMath. To further substantiate
 733 this claim, we extract and compare sample instances from both datasets to illustrate their differences.
 734 OpenWebMath and GSM8K differ significantly in format, content, and purpose. OpenWebMath is
 735 a large-scale, web-crawled mathematical text corpus designed for pretraining, containing a mix of
 736 continuous mathematical content (e.g., LaTeX equations, proofs). In contrast, GSM8K is a curated
 737 dataset of grade-school-level math word problems, formatted as question-answer pairs with explicit
 738 step-by-step reasoning.

739 Table 4 shows the significant differences between OpenWebMath and GSM8K. The performance
 740 degradation on GSM8K may be attributed to the following potential factors based on our analysis:

- 742 • Pretraining on OpenWebMath may inadequately prepare models for GSM8K’s task-
 743 specific format.
- 744 • OpenWebMath’s focus on declarative mathematical knowledge might not transfer to
 745 GSM8K’s procedural reasoning demands.
- 746 • Models pretrained on continuous text may struggle with GSM8K’s segmented Q&A struc-
 747 ture, lacking fine-tuned alignment for answer generation.

748 We use a heatmap to show the relationship between the ratios of pre-training data sources (general,
 749 code, and math) and downstream tasks under GRPO. As illustrated in Figure 5, it can be clearly ob-
 750 served that increasing the ratios of Math to General, Code to General, and Code to Math data leads to
 751 positive effects on most tasks except for the Math-related tasks. In other words, a higher proportion
 752 of math-domain pre-training data tends to degrade performance on the GSM8K task. This ob-
 753 servation supports our hypothesis that there exists a noticeable gap between OpenWebMath (which is
 754 more oriented toward theorems and proofs) and GSM8K&Math (which focuses more on arithmetic
 755 operations such as addition and subtraction) in terms of data format and knowledge coverage.

756	Dataset	Sample
757	OpenWebMath	Question: What is the derivative of $f(x) = (e^{2x})(\ln(x))$? $f'(x) = e^{2x} \left(2 \ln x + \frac{1}{x}\right)$ Explanation: The derivative of $\ln x$ is $\frac{1}{x}$ The derivative of $e^g(x)$ is $e^g(x) \cdot g'(x)$ The derivative of $h(x) \cdot l(x)$ is $h'(x) \cdot l(x) + h(x) \cdot l'(x)$ Then $f'(x) = e^{2x} \cdot 2 \cdot \ln x + e^{2x} \cdot \frac{1}{x} = e^{2x} \left(2 \ln x + \frac{1}{x}\right)$
758		Answer:
759	GSM8K	Question: Bella has two times as many marbles as frisbees. She also has 20 more frisbees than deck cards. If she buys 2/5 times more of each item, what would be the total number of the items she will have if she currently has 60 marbles? Let's think step by step. When Bella buys 2/5 times more marbles, she'll have increased the number of marbles by $2/5 * 60 = 24$. The total number of marbles she'll have is $60 + 24 = 84$. If Bella currently has 60 marbles, and she has two times as many marbles as frisbees, she has $60/2 = 30$ frisbees. If Bella buys 2/5 times more frisbees, she'll have $2/5 * 30 = 12$ more frisbees. The total number of frisbees she'll have will increase to $30 + 12 = 42$. Bella also has 20 more frisbees than deck cards, meaning she has $30 - 20 = 10$ deck cards. If she buys 2/5 times more deck cards, she'll have $2/5 * 10 = 4$ more deck cards. The total number of deck cards she'll have is $10 + 4 = 14$. Together, Bella will have a total of $14 + 42 + 84 = 140$ items. The answer is 140.
760		Answer:

Table 4: Samples from OpenWebMath and GSM8K.

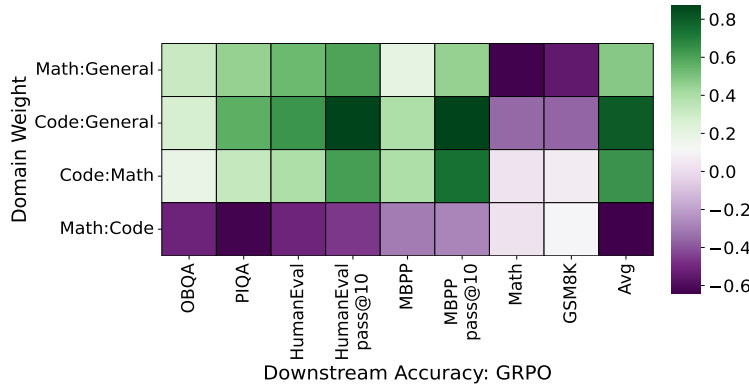


Figure 5: The relationship between the ratios of pre-training data sources (general, code, and math) and downstream tasks under GRPO.

D SUPPLEMENTARY EXPERIMENTS

D.1 ANALYSIS OF THE FITTED LIGHTGBM PERFORMANCE ON PREDICTING THE DATA MIXTURE

We further explore the performance of the best-performing regression model (LightGBM) across a broader space, where the training data is generated based on GRPO RL algorithm. Figure 6 illustrates the simulated new data mixtures alongside the corresponding predicted targets to find the best data mixture. As can be seen from the figure, when the regression model achieves its optimal target value, the proportions of code and math data are relatively low.

D.2 THE IMPACT OF PREDICTED MIXTURE ON DOWNSTREAM TASKS UNDER THE DPO ALGORITHM

We further validate the efficacy of Go4RL on downstream reasoning tasks under DPO. We compare the Go4RL predicted data mixture with three baselines: Random, RL_loss and Worst. Random randomly selects five distinct data mixtures to train models following the pre-training + RL pipeline, and the average performance of these five models is reported as the final result. Refer to the details of other baselines in experimental setups. At first, we utilize Go4RL to predict the top 5 best data mixture strategies. Then We train 1B parameter-based models using the predicted data mixture and use DPO to get RL-trained models separately. Table 5 lists the average score of 3 runs for the top-5 best 1B RL-trained models selected by Go4RL.

Table 5 shows that pretraining data mixtures using the proposed optimization objective $\text{avg}(k\text{-ppl})$ have an obvious impact on reasoning downstream tasks. Compared to the three baselines, Go4RL

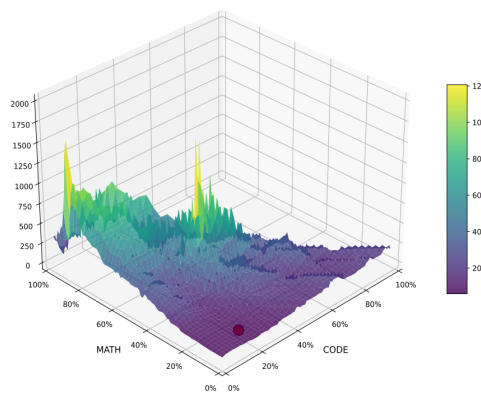


Figure 6: Simulate potential data mixtures across a broader space and use the regression model to predict the best data mixture (lowest avg(k-ppl) marked with the red dot).

Table 5: Average performance of 1B models trained by DPO, using the top-5 best data mixtures selected by Go4RL, compared with several other data selection baselines. BSET ON indicates how many of all tasks the model achieves the best results in. The reported performance on each task is the average score of 3 runs, while the highest score on each task is highlighted in bold.

Baselines	Tasks	General			Code		Math		Avg.	Best On
		OBQA	PIQA	Hellaswag	Humaneval	MBPP	MATH	GSM8K		
		Acc.	Acc.	Acc.	Pass@10	Pass@10	Acc	Acc		
Random	OBQA	7	14.8	20.5	14.0	1.0	0.5	0.1	8.3	0
Human	PIQA	8.6	6.9	22.5	20.1	2.8	0.6	2.0	9.1	1
RL_loss	Hellaswag	7.6	28.6	22.5	29.3	10.4	0.8	0.2	14.2	1
Go4RL	Worst	18.6	16.5	24.5	29.9	10.8	0.7	0.4	14.5	2
Go4RL	Best	12.5	18.6	24.5	36.6	11.1	1.0	0.7	15.0	4

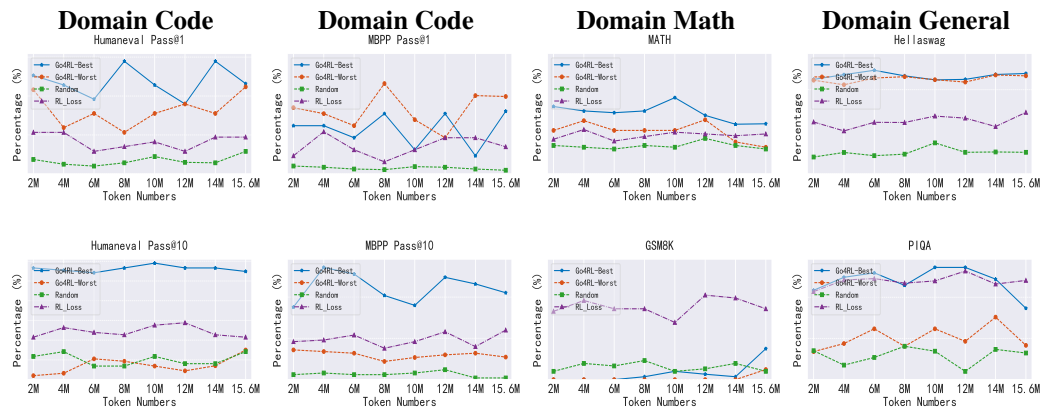
demonstrates a superior performance, outperforming all three competing baselines in 4 out of 7 tasks while achieving the highest average score. The average performance improvement across all the tasks highlights both the crucial role of data mixtures in the pretraining+RL pipeline and the validity of our data selection method. The RL_loss baseline also exhibits suboptimal performance under DPO, indicating that the RL loss function alone is insufficient as an evaluation metric for the pre-train+RL pipeline. These results from both GRPO and DPO demonstrate that Go4RL serves as a versatile framework for selecting data mixture ratios. Regardless of the reinforcement learning algorithm used, models trained with Go4RL consistently achieve superior average performance across downstream tasks in various domains.

We also observe a performance decline on general tasks. A potential explanation is that the training data used in the RL phase exhibits a stronger bias toward in-domain content, thereby narrowing the reasoning capacity of the base model, which is a phenomenon consistent with prior research (Yue et al., 2025). This also indicates the complexity of the relationship between pre-training and RL, which needs further exploration.

D.3 HOW DOES THE PERFORMANCE OF MODELS WITH DIFFERENT DATA MIXTURES IMPROVE DURING RL UNDER GRPO?

We are interested in how the RL-trained models favor the domain distribution with the accumulated RL steps. As shown in Figure 7, we compare trajectories during RL of the models pretrained with data mixtures selected by Go4RL (top-5 best) with the random sampling, RL_loss and Go4RL-worst baselines. For the code domain, we compare the pass@k (k=1,10) trajectories over MPBB and Humaneval benchmarks. Go4RL-best demonstrates strong RL gains from the starting point, eventually achieving the largest RL reasoning gains for almost all the pass@1 and pass@10 evaluations. For the MATH benchmark, Go4RL-best consistently maintains a significant lead throughout the training process. On the PIQA benchmark, Go4RL and RL_Loss achieve comparable performance, with both methods consistently maintaining a leading position.

864 Like the results of DPO, these results also prove that the performance in the RL phase is not the sole
 865 factor affecting downstream knowledge expression and generation. Finding a suitable base model
 866 also plays a significant role.
 867



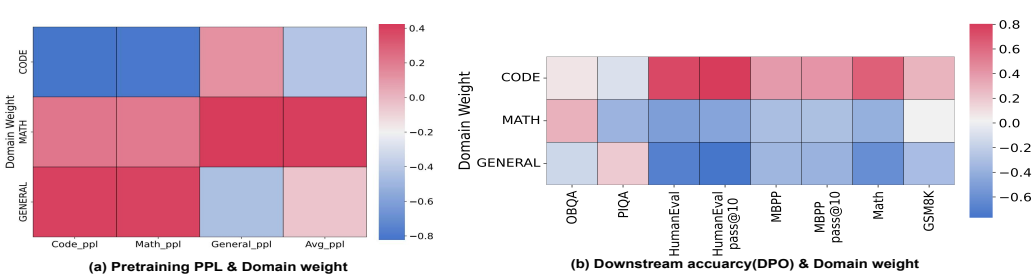
883 Figure 7: Three domains' downstream performances of the Go4RL-optimal 1B parameter models
 884 with top-5 best data mixtures, compared with the random sampling method, RL.loss and Go4RL-
 885 worst baselines under GRPO algorithm. The x-axis is the growing training tokens in the RL stage.
 886
 887

888 D.4 WHAT'S A PROPER MEASUREMENT FOR THE DATA MIXTURES TARGETING RL 889 PERFORMANCE?

891 In addition, we visualize the correlation between the potential measurement of downstream task
 892 accuracy and the different data domains under the DPO.

893 For the downstream tasks illustrated in Figure 8(b), beyond general-domain benchmarks such as
 894 OBQA and PIQA, the proportion of code data exhibits a positive correlation with performance on
 895 most downstream tasks. This outcome is particularly evident on the HumanEval benchmark, which
 896 aligns well with our intuitive expectations. An increase in the proportion of math data proves ben-
 897 efitical to the performance on the OBQA task to some extent, demonstrating that enhanced mathe-
 898 matical capability can effectively improve the model's logical reasoning and structured expression
 899 abilities. The visualization results highlight the importance and inherent complexity of determin-
 900 ing the optimal pre-training data mixture and give hints for the further improvement of the Go4RL
 901 method.

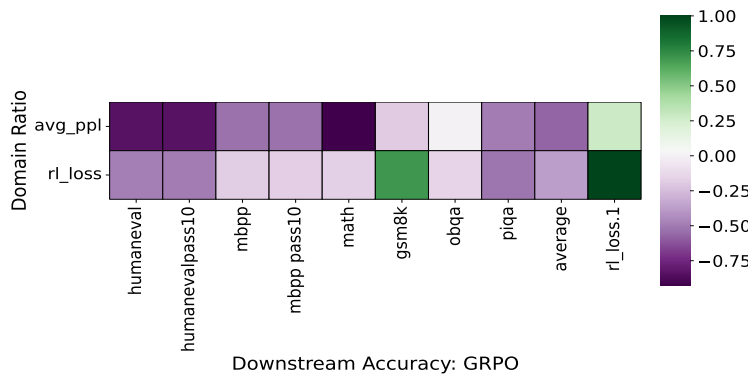
902 The visualization results highlight the importance and inherent complexity of determining the opti-
 903 mal pre-training data mixture and give hints for the future improvement of the Go4RL method.
 904



914 Figure 8: (a) The correlations between avg(k-ppl) and training data ratios across three domains
 915 separately and averaged over 1B models. (b) The correlations between downstream accuracy and
 916 training domain ratios on 1B models.
 917

918 D.5 IS IT WORTH USING THE PROXY MODELS?
919920 We report the GPU hours and FLOPs required to fit 512 1M-parameter models for predicting the
921 optimal data mixtures, and compare them against other baselines. As listed in the Table 6, the
922 computational cost of our approach remains within an acceptable and marginal range.
923924 Our target is to predict the optimal data mixture for larger base models, thereby saving the cost of
925 retraining the base models to get the optimal one. When compared to the entire cost of training a 1B
926 base model on 25B tokens, training proxy models is rather inexpensive—only roughly 5%. The ef-
927 fect would be significantly greater when the training data and base model parameters are increased.
928 Therefore, the choice of proxy models should be viewed as a trade-off between computational effi-
929 ciency and final model performance.
930931 Table 6: Computational consumption of Go4RL, compared with other baselines.
932

Method	PPL		Human	Go4RL		
	Stage	Pre-training		Pre-training	RL	Total
FLOPs	1.95E+19	7.45E+19	0	3.07E+18	7.14E+19	7.45E+19
GPU hours	4.08	16.14	0	0.64	15.5	16.14

937 D.6 WHY IS AVG(K-PPL) SUPERIOR TO OTHER FITTING TARGETS?
938939
940 **RL_loss:** We further analyze the correlation between avg(k-ppl) and RL_loss with downstream tasks,
941 as well as the correlation between avg(k-ppl) and RL_loss themselves, to substantiate why we choose
942 avg(k-ppl) as the fitting target.
943944 The higher the correlation between metrics, the larger the absolute value. As shown in Figure 9,
945 choosing avg(k-ppl) as the target for fitting yields noticeably greater advantages and gains on down-
946 stream tasks compared to directly fitting the RL loss ($| -0.57 | > | -0.37 |$). Additionally, the pos-
947 itive correlation between avg-ppl and RL loss ($value = 0.35$) indicates that avg(k-ppl) and RL_loss
948 influence the model in the same direction. These empirical factors make avg(k-ppl) our first choice
949 for fitting the regression model.
950951
952
953
954
955
956
957
958
959
960
961
962
963 Figure 9: The correlations between avg(k-ppl) and RL_loss with downstream tasks over 1B models,
964 under GRPO algorithm.
965966 **avg(k-entropy):** We also conduct experiments with the same settings to compare the fitting targets
967 avg(k-entropy) with avg(k-ppl). The experimental results are listed in Table 7. According to the
968 results, avg(k-ppl) surpasses the entropy metrics in downstream tasks.
969970 **downstream metrics:** Using the downstream metrics, like the pass@k metric could also evaluate
971 the performance. However, we argue that using downstream-task pass@k as the regression target
972 may introduce several inherent limitations:
973

972 Table 7: Average performance of 1B models trained by GRPO, using the top-5 best data mixtures
 973 selected by Go4RL, compared with avg(k-entropy). BSET ON indicates how many of all tasks the
 974 model achieves the best results in. The reported performance on each task is the average score of 3
 975 runs, while the highest score on each task is highlighted in bold.
 976

Domain	General			Code		Math		Avg.	Best On
Tasks	OBQA	PIQA	Hellaswag	Humaneval	MBPP	MATH	GSM8K		
avg(k-entropy)	16.2	10.6	24.9	4.3	0	0.2	2.3	8.4	2
avg(k-ppl) (Go4RL)	12.5	21.2	25.3	36.8	10.5	1.1	0.9	15.5	5

977

978

979

980

981

982

983

984

985

986

987

988

989

990

991

992

993

994

995

996

- High Noise and Instability: pass@k is inherently a discrete and high-variance metric, particularly on code, math, or multi-step reasoning tasks with limited evaluation samples, which injects significant noise into the regression targets and weakens the regressor’s ability to learn stable performance trends.
- Strong nonlinearity with limited samples: The relationship between pass@k and the model’s true capability is often highly nonlinear and even piecewise. The regression model may struggle to capture this structure, leading to underestimation of improvements in some regions or overestimation of gains in the high-performance regime.
- Lack of Generalizable Capability: Using pass@k as the regression target effectively ties the objective to a particular task, prompt format, and evaluation configuration. As a result, the inferred optimal data mixture may overfit to idiosyncrasies of that specific downstream task, and therefore may not generalize well to other tasks or to large-scale RL training.

D.7 CAN GO4RL BE EXTENDED TO A LARGER MODEL?

999 To further validate the feasibility of applying Go4RL to larger-scale models, we train 300 proxy
 1000 models with 60M parameters each on 1B tokens, fit a regression model, and use the regression
 1001 model’s predicted data mixtures to guide the training of a 3B parameter model.

1002 As shown in Table 8, the regression model achieves 68.23% in the ρ metric, demonstrating that
 1003 Go4RL can scale effectively to larger models. When the target model becomes larger, using proxy
 1004 models with more parameters leads to higher prediction accuracy in the fitted regression model,
 1005 which aligns with our intuition. Therefore, selecting the proxy model size requires balancing com-
 1006 putational budget against performance gains, depending on the practical constraints of the computa-
 1007 tional sources.

1009 Table 8: We separately fit three regression models based on the results of the 60M parameter models
 1010 trained on 1B tokens and validate them on unseen data mixtures for 60M and 1B parameter models.
 1011 ρ compares the predicted and actual data mixtures.

	60M>60M	60M>3B
Metric	ρ	ρ
lightGBM	77.85	68.23

D.8 IS GO4RL STABLE UNDER DIFFERENT SAMPLING SETTINGS?

1020 We conduct further experiments over different sampling settings, including k values and random
 1021 seeds. As shown in Table 9, the variation of the settings shows that the ρ values, which indicate
 1022 regression performance, remain relatively stable.

1026
 1027
 1028
 1029
 1030
 1031
 1032
 1033
 1034
 1035
 1036
 1037
 1038
 1039
 1040
 1041
 1042
 1043
 1044
 1045
 1046
 1047
 1048
 1049

Table 9: ρ compares the predicted and actual data mixtures, under different sampling settings.

Method		$\rho(\mathbf{IM} \rightarrow \mathbf{IM})$
k-value	k=32	87.82
	k=128	86.46
random_seeds	seeds = 1234	85.23
	seeds = 4321	86.19

1050
 1051
 1052
 1053
 1054
 1055
 1056
 1057
 1058
 1059
 1060
 1061
 1062
 1063
 1064
 1065
 1066
 1067
 1068
 1069
 1070
 1071
 1072
 1073
 1074
 1075
 1076
 1077
 1078
 1079